

## Spin-coated Ga-doped ZnO transparent conducting thin films for organic light-emitting diodes

This article has been downloaded from IOPscience. Please scroll down to see the full text article.

2009 J. Phys. D: Appl. Phys. 42 139801

(<http://iopscience.iop.org/0022-3727/42/13/139801>)

[The Table of Contents](#) and [more related content](#) is available

Download details:

IP Address: 147.46.118.89

The article was downloaded on 10/11/2009 at 06:40

Please note that [terms and conditions apply](#).

# Corrigendum

## **Spin-coated Ga-doped ZnO transparent conducting thin films for organic light-emitting diodes**

Pradipta K Nayak, Jihoon Yang, Jinwoo Kim, Seungjun Chung, Jaewook Jeong, Changhee Lee and Yongtaek Hong 2009 *J. Phys. D: Appl. Phys.* **42** 035102

Two corrections should be made to the previously published version of this article.

On page 1, right-hand column, the radius of Zn should be read as 0.074 nm. This value is taken from Lide D R 1991 *Handbook of Chemistry and Physics* 71st edn (Boca Raton, FL: CRC Press).

In the first paragraph of section 2, Diethanolamine and its acronym DEA should be corrected to Monoethanolamine and MEA.

**The original text follows this page**

# Spin-coated Ga-doped ZnO transparent conducting thin films for organic light-emitting diodes

Pradipta K Nayak, Jihoon Yang, Jinwoo Kim, Seungjun Chung,  
Jaewook Jeong, Changhee Lee and Yongtaek Hong

School of Electrical Engineering, Seoul National University, San 56-1 Shinlim-Dong, Kwanakgu,  
Seoul 151-744, Korea

E-mail: [yongtaek@snu.ac.kr](mailto:yongtaek@snu.ac.kr)

Received 9 September 2008, in final form 19 November 2008

Published 18 December 2008

Online at [stacks.iop.org/JPhysD/42/035102](http://stacks.iop.org/JPhysD/42/035102)

## Abstract

Gallium doped zinc oxide (GZO) thin films have been prepared by a simple sol-gel spin coating technique. XRD results showed the preferential *c*-axis orientation of the crystallites and the presence of the wurtzite phase of ZnO. A lowest resistivity of  $3.3 \times 10^{-3} \Omega \text{ cm}$  was obtained for the ZnO film doped with 2 at% of Ga after post-annealing at 500 °C for 45 min in a H<sub>2</sub> atmosphere. All the films showed more than 80% of transparency in the entire visible region. Blue shifting of the optical band gap was observed with an increase in Ga doping, which can be explained on the basis of the Burstein-Moss effect. OLED devices were fabricated using 2 at% Ga-doped ZnO thin films as anodes. Preliminary results obtained demonstrated that spin-coated GZO films can be used as a promising TCO for optoelectronic device applications.

(Some figures in this article are in colour only in the electronic version)

## 1. Introduction

In recent years, transparent conducting oxide (TCO) thin films have attracted much attention due to their potential applications in displays, solar cells, surface acoustic wave devices, piezoelectric transducers, gas sensors, phosphors and other optoelectronic devices [1, 2]. Tin doped indium oxide (ITO) is indeed the most widely used TCO for flat panel display (FPD) or solar cell applications. However, indium is a very expensive material and ITO is less stable in hydrogen plasma. Therefore, impurity doped zinc oxide (ZnO), such as Al or Ga-doped ZnO, has recently gained much attention [3–7] as an alternative material to ITO. Pure and impurity doped ZnO thin films have several advantages such as low resistivity, high transmittance in the visible range, abundance in natural resource and stability under exposure to hydrogen plasma.

Zinc oxide is a wide band gap (3.3 eV) n-type semiconductor with hexagonal wurtzite structure. Although Al-doped ZnO (AZO) is an attractive electrode material alternative to ITO, Ga-doped ZnO (GZO) is more stable with

respect to oxidation due to gallium's greater electronegativity in comparison with aluminium [8]. It has also been reported that heavily Ga-doped ZnO is more stable when subjected to moisture than Al-doped ZnO [9]. Moreover, recent studies have reported the use of ZnO as an air stable anode in an OLED providing additional evidence of GZO as a promising TCO for organic device applications [10]. It is believed that the introduction of Ga can increase free electron density by replacing the host atoms (Zn) [11]. The substitution of Ga is possible due to the smaller radius of Ga (0.062 nm) compared with Zn (0.083 nm). Several approaches have been proposed and developed for the preparation of Ga-doped ZnO thin films such as magnetron sputtering [12], spray pyrolysis [13], metal-organic chemical vapour deposition (MOCVD) [14], pulsed laser deposition (PLD) [15–17], arc plasma evaporation [18], dip-coating [19] and ion plating [20]. In comparison with the above thin film preparation techniques, the sol-gel spin coating method has distinct advantages such as cost effectiveness, simplicity, homogeneity, excellent compositional control at the molecular level and lower crystallization temperature. Moreover, high deposition

rate and easier incorporation of dopants make this technique suitable for frontier research.

In this work, we report the structural, optical and electrical properties of the transparent conducting GZO thin films prepared by a simple sol–gel spin coating method. Further, organic light-emitting diode (OLED) devices were fabricated using the GZO thin films as anodes and their current density–luminance–voltage characteristics were investigated.

## 2. Experimental details

The precursor solution for spin coating was prepared by dissolving an appropriate amount of zinc acetate dihydrate and gallium nitrate in 2-methoxyethanol at room temperature. Diethanolamine (DEA) was then added to the mixture as the sol stabilizer. The concentration of gallium was varied from 0 to 5 at%. The total concentration of the sol was maintained at  $0.5 \text{ mol L}^{-1}$  and the molar ratio of DEA to zinc acetate was maintained at 1.0. The resulting mixture was then stirred at  $50^\circ\text{C}$  for 1 h to form a clear and transparent homogeneous mixture. The precursor solution was aged for 48 h at room temperature. The glass substrates (Eagle 2000) were cleaned thoroughly with acetone, isopropanol and finally with deionized water with the help of an ultrasonic bath. The films were obtained by spin coating the sol at a rotation speed of 3000 rpm for 30 s. The wetted films were dried at  $350^\circ\text{C}$  for 15 min. The process of coating and subsequent drying at  $350^\circ\text{C}$  was repeated 10 times in order to get a film of the desired thickness. Finally, the films were annealed at  $600^\circ\text{C}$  for 1 h in air. The as-prepared films were post-annealed in a hydrogen atmosphere using forming gas (4.2%  $\text{H}_2$  and 95.8%  $\text{N}_2$ ) at  $500^\circ\text{C}$  for 45 min for further improvement in electrical properties.

X-ray diffraction (XRD) studies were performed by a PANalytical X'Pert PRO powder diffractometer using  $\text{Cu K}\alpha$  radiation. The surface morphology of the films was examined by a field emission scanning electron microscope (Philips, XL30-FEG). The thickness of the films was measured by a KLA-TENCOR Alfa-step 500 (Nanospec AFT/200) profilometer. In all cases, the thickness of the films was found to be  $\sim 300 \text{ nm}$ . The sheet resistance and hence the resistivity of the films were measured using a LS SYSTEM INC. (4P-R) four point probe system. Transmittance spectra of the films were recorded by a Beckman (DU<sup>®</sup>-70) UV–VIS spectrophotometer. A Jobin-Yvon HR460 monochromator and a Kimmon He–Cd laser ( $\lambda = 325 \text{ nm}$ ) were used for photoluminescence (PL) studies.

For OLED device fabrication, glass substrates coated with 2 at% Ga-doped ZnO thin films (thickness  $\sim 300 \text{ nm}$ ) were used as anodes. Prior to device fabrication, the GZO anodes were first defined by using a patterned Kapton tape based etch mask on the film and diluted HCl as an etchant and then the patterned GZO anodes were exposed to the UV ozone for 5 min. The device structure consisted of Al/LiF as the cathode, tris(8-hydroxyquinolinolato)aluminium(III) ( $\text{Alq}_3$ ) as the emitting layer, *N,N'*-di-[(1-naphthyl)-*N,N'*-diphenyl]-(1,1'-biphenyl)-4,4'-diamine ( $\alpha$ -NPD) as the hole transporting layer

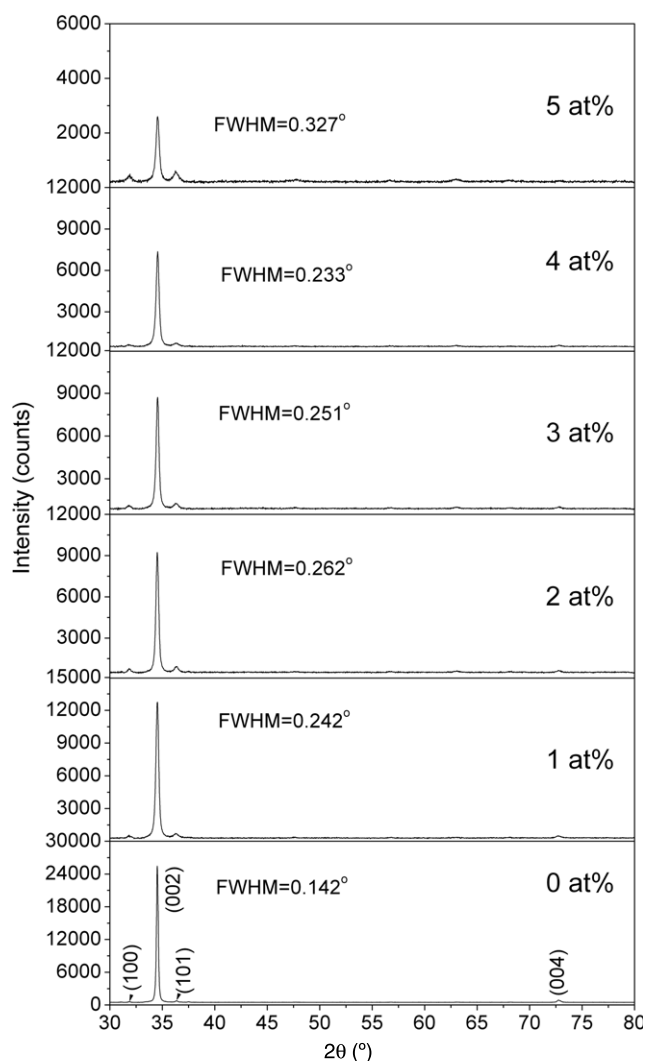


**Figure 1.** XRD patterns of the as-prepared ZnO thin films doped with different gallium concentrations. The intensity of the (002) peak decreases with incorporation of gallium in the films.

and 4,4', 4''-tris[3-methylphenyl (phenyl)amino]triphenylamine (m-MTDATA) as the hole injection layer. All the organic layers and cathode layer was thermally evaporated using shadow masks. All the fabricated OLEDs were encapsulated by using cap glasses. The current density–voltage–luminance characteristics were measured with a Keithley 236 source-measure unit and a Keithley 2000 multimeter equipped with a PMT through an ARC 275 monochromator and a calibrated Si photo diode in a dark room. All the characterizations were performed at room temperature in air.

## 3. Results and discussions

Figure 1 shows the XRD patterns of the as-prepared ZnO thin films doped with different Ga concentrations. All the films show the existence of a very strong peak corresponding to (002) and weak peaks corresponding to (100), (101), (004) reflections of the wurtzite phase of ZnO. The strong and dominating nature of the peak corresponding to the

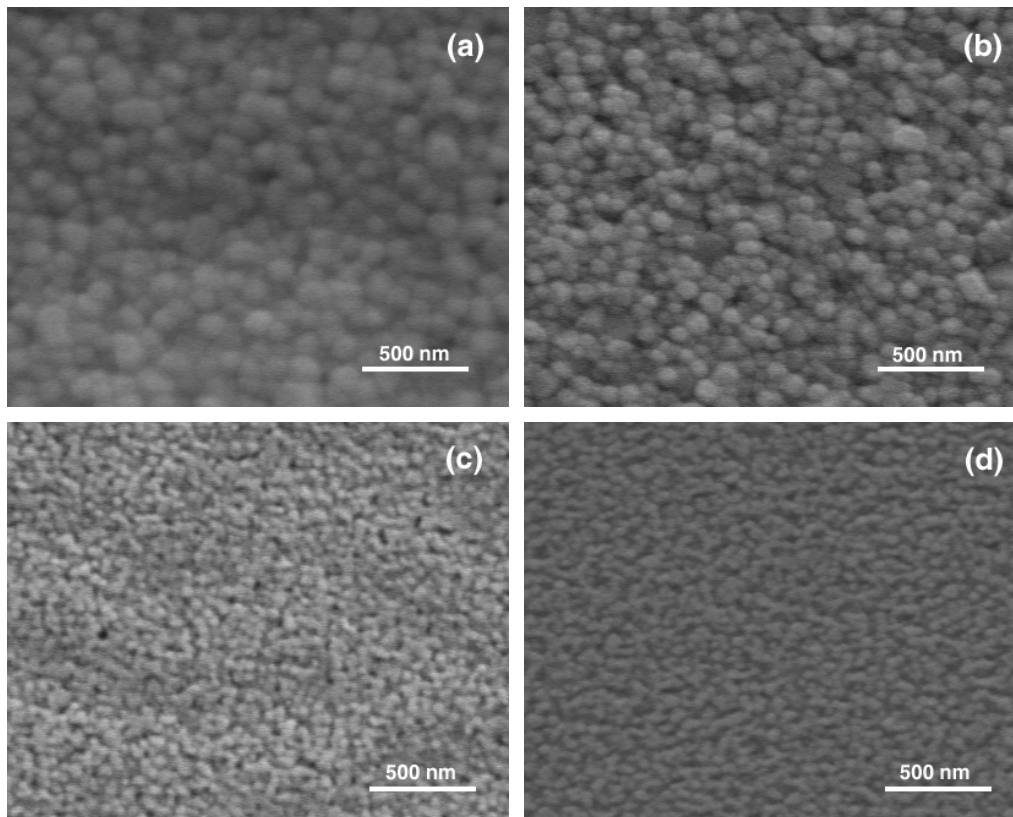


**Figure 2.** FE-SEM images of GZO thin films with (a) 0 at%, (b) 1 at%, (c) 2 at% and (d) 5 at% of gallium. The average grain size decreases with incorporation of gallium in the film.

(002) reflection indicates the preferential *c*-axis orientation of crystallites. Moreover, the intensity of the (002) peak decreased significantly with 1 at% of Ga incorporation in the film and it gradually decreased with a further increase in the Ga content in the films. This behaviour indicates that the increase in the doping concentration deteriorates the crystallinity of the films, which may be attributed to the influence of stresses arising due to the difference in the ionic radii of zinc and gallium [21]. It is also observed that the full width at half maximum (FWHM) of the peak corresponding to the (002) reflection increased with Ga incorporation in the films. The crystallite sizes calculated using Scherrer's formula for ZnO films with 0 at%, 1 at%, 2 at%, 3 at%, 4 at% and 5 at% of Ga were found to be 59 nm, 34 nm, 32 nm, 33 nm, 35 nm and 25 nm, respectively. It is noted that the instrumental broadening effect has been removed by using the XRD pattern of a standard silicon sample.

Figure 2 shows the FE-SEM images of the ZnO thin films doped with different concentrations of Ga. The average grain size in the case of the undoped ZnO film was found to be 125 nm. However, the size of the grains decreased with incorporation of Ga in doped films. The average grain sizes in the case of 1 at%, 2 at% and 5 at% of Ga-doped ZnO films were found to be 100 nm, 55 nm and 50 nm, respectively. The decrease in grain size with Ga doping is well corroborated by the XRD results. However, the grain sizes calculated from the FE-SEM images are larger than the values obtained from the XRD data. Similar results and tendency have also been observed by Mridha and Basak [22] for aluminium doped ZnO

films. They reported that the grain size extracted from the FE-SEM images was larger because smaller crystallites were attached together to form larger grains which were imaged by FE-SEM.

The UV-VIS transmittance spectrum and the  $\alpha^2$  versus  $h\nu$  plot of the as-prepared GZO thin films are shown in figure 3. The undoped ZnO film shows a transparency of more than 80% in the spectral range of 400–700 nm. There was a slight variation in the transparency for different amounts of Ga doping. The optical absorption coefficient  $\alpha$  can be obtained through  $I = I_0e^{-\alpha t}$ , where  $I$  and  $I_0$  are the intensities of the transmitted light and the incident light, respectively, and  $t$  is the thickness of the GZO film. In the direct transition semiconductor, the absorption coefficient ( $\alpha$ ) follows the following relationship with optical band gap ( $E_g$ );

$$\alpha h\nu = B(h\nu - E_g)^{1/2}, \quad (1)$$

where  $h$  is Planck's constant,  $\nu$  is the frequency of the incident photon and  $B$  is a constant which depends on the electron-hole mobility. The optical band gap can be determined by extrapolation of the linear region from the  $\alpha^2$  versus  $h\nu$  plot (figure 3(b)) near the onset of the absorption edge to the energy axis. The band gap of the undoped ZnO film was found to be 3.28 eV, which agrees well with the bulk band gap of ZnO. Further, it is clearly seen that the absorption onset of Ga-doped films is slightly blue shifted from undoped ZnO. The blue shift of absorption onset is associated with the increase in the carrier concentration blocking the lowest states in the conduction band, well known as the Burstein-Moss effect [23, 24].

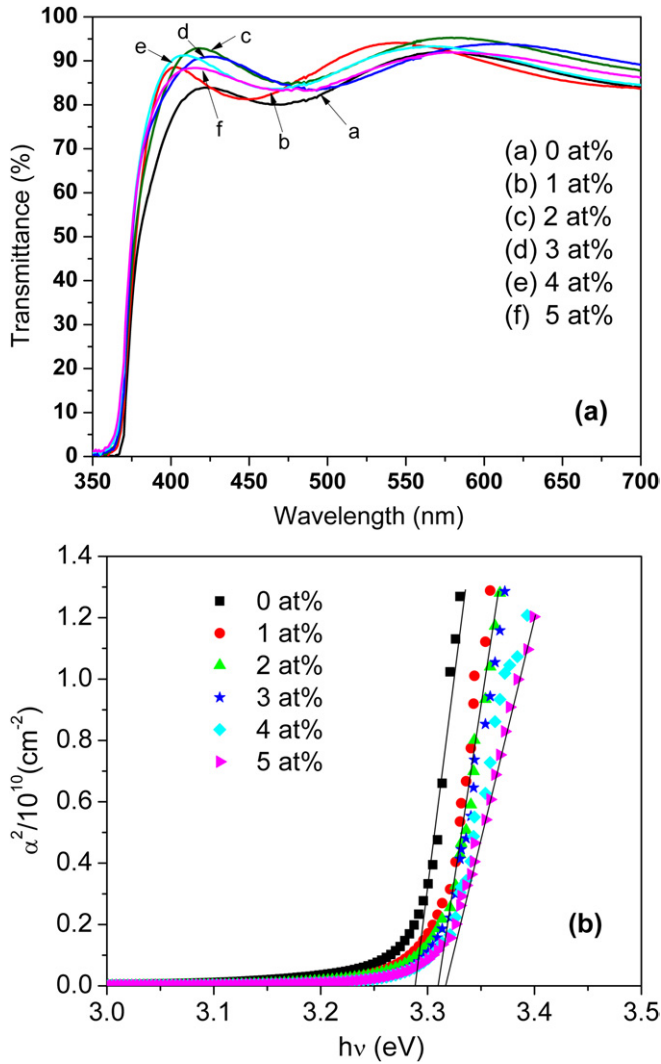


**Figure 3.** (a) Transmittance spectra and (b) the  $\alpha^2$  versus  $h\nu$  plot of the ZnO thin films doped with different gallium concentrations. The absorption onset is blue shifted with the increase in the Ga concentration in the film due to the Burstein–Moss effect.

PL spectra of the GZO thin films are shown in figure 4. The PL spectra for all the GZO films show an intense and sharp peak at  $\sim 3.28$  eV due to excitonic recombination corresponding to band-edge emission. The intensity of the band-edge emission peak gradually decreases with the increase in Ga content in the films. Similar behaviour has also been observed by Kaul *et al* [14] for Ga-doped ZnO prepared by MOCVD. The PL spectrum of the undoped ZnO film shows a very broad feature below  $\sim 2.4$  eV due to the presence of interstitial oxygen defects in ZnO films [25]. However, the broad feature disappears in the case of Ga-doped ZnO films, which may be due to the consumption of interstitial oxygen by  $\text{Ga}^{3+}$  ions.

Figure 5 shows the sheet resistance of the as-prepared GZO films and  $\text{H}_2$  annealed with different Ga concentrations. The sheet resistance for the as-prepared undoped ZnO film was found to be  $1.86 \text{ M}\Omega/\square$  (resistivity;  $55.8 \Omega \text{ cm}$ ). However, the sheet resistance was significantly decreased with the incorporation of Ga in the films. A lowest sheet resistance of  $32.0 \text{ k}\Omega/\square$  (resistivity;  $0.96 \Omega \text{ cm}$ ) was obtained for the ZnO films doped with 2 at% of Ga. The decrease in the sheet

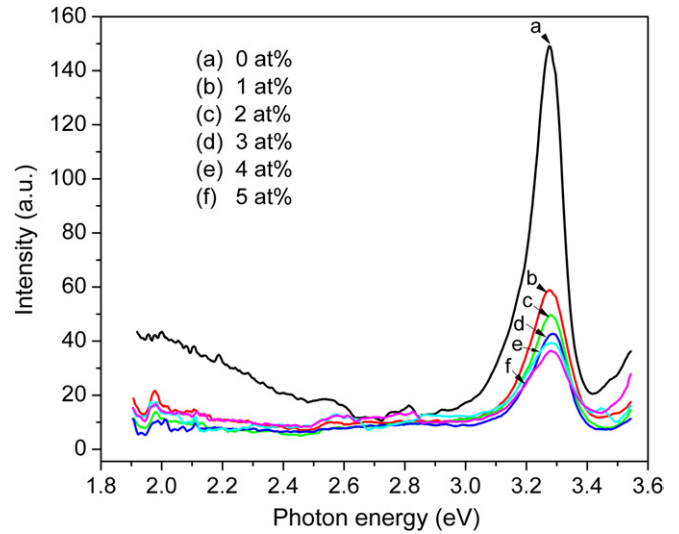


**Figure 4.** PL spectra of the ZnO thin films doped with different gallium concentrations. The intensity of the band-edge emission at  $\sim 3.28$  eV decreases with incorporation of gallium in the film. The broad feature below  $\sim 2.4$  eV of the undoped film disappeared with gallium incorporation because of the consumption of interstitial oxygen defects by  $\text{Ga}^{3+}$  ions.

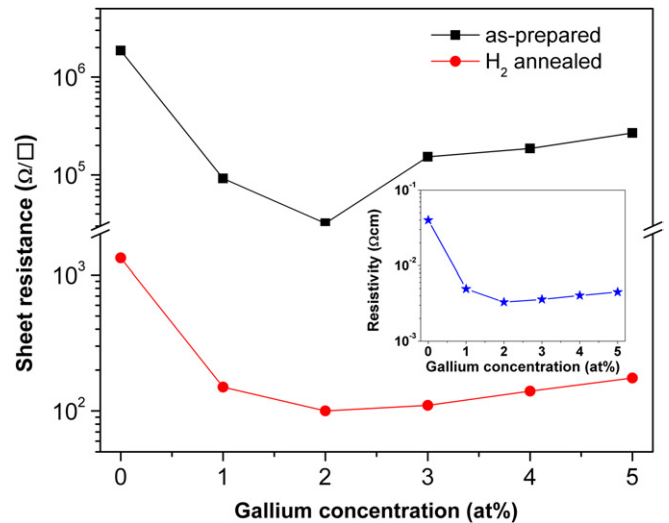


**Figure 5.** Variation of the sheet resistance of as-prepared and  $\text{H}_2$ -annealed GZO thin films with different Ga concentrations. The inset shows the resistivity of the GZO thin films after  $\text{H}_2$  annealing.

resistance in the case of doped films is due to the increase in carrier concentrations supplied from the substitution of Ga by replacement of the host Zn atoms. The substituted Ga atoms ionize into  $\text{Ga}^{3+}$  so that a free electron can be contributed from each Ga atom [11]. These results corroborate well with the blue shifting of the optical band gap as observed from the  $\alpha^2$  versus  $h\nu$  plot. However, a slight increase in the sheet resistance was observed with the increase in the Ga concentration above 2 at%. At higher Ga concentrations, the carrier concentration decreases because increasing the dopant atoms may cause segregation of neutral Ga atoms at the grain boundaries which do not contribute free electrons.

The as-prepared films were post-annealed at  $500^\circ \text{C}$  in a  $\text{H}_2$  atmosphere for 45 min to further reduce the sheet resistance

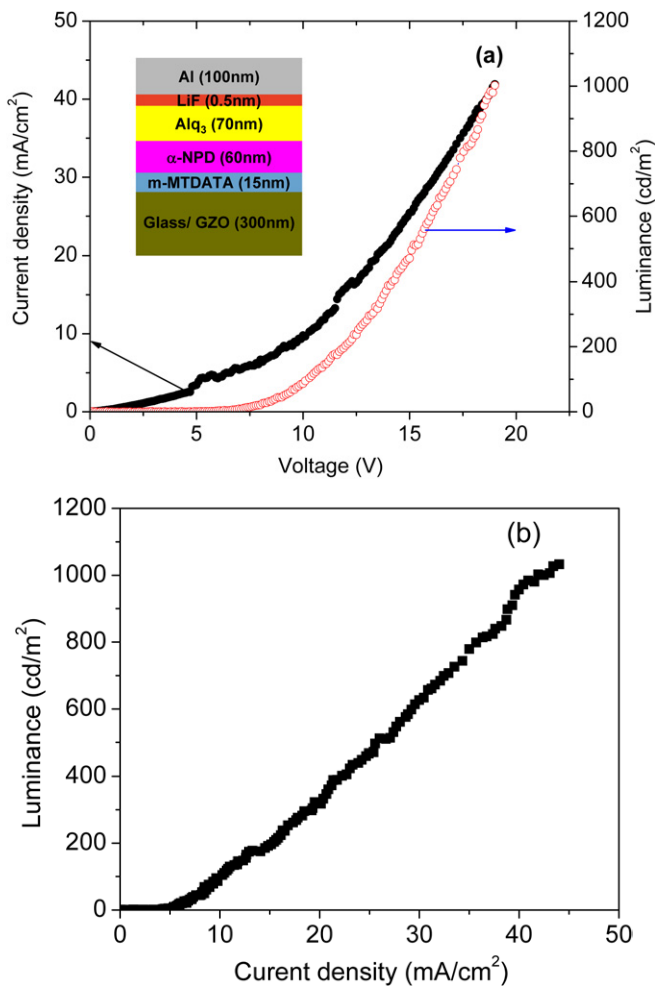


**Figure 6.** (a) Current density–voltage–luminance ( $J$ – $V$ – $L$ ) and (b) current density–luminance ( $J$ – $L$ ) characteristics of the device schematically represented in (a). Lower performance of the OLED partially comes from the lower work function of GZO or increase in the sheet resistance after GZO films were patterned.

and hence the resistivity. The electrical conductivity of ZnO is believed to be controlled by zinc interstitials [26] and/or oxygen vacancies [27] which act as n-type donors. Hydrogen acts as a reducing agent and hence an oxygen deficient non-stoichiometric ZnO film is produced after  $\text{H}_2$  annealing. Therefore, the decrease in resistivity by  $\text{H}_2$  annealing may be due to zinc interstitials and/or oxygen vacancies [28] in the films. As shown in figure 5, the sheet resistance of the GZO films was reduced by two orders of magnitude after annealing in a  $\text{H}_2$  atmosphere. The lowest sheet resistance of  $110 \Omega/\square$  (resistivity;  $3.3 \times 10^{-3} \Omega \text{ cm}$ ) was obtained for the films with 2 at% of Ga. The obtained minimum resistivity for the ZnO films with 2 at% Ga is very similar to the resistivity value ( $6.3 \times 10^{-3} \Omega \text{ cm}$ ) reported by Fathollahi and Amini [19] for the 2 at% Ga-doped ZnO film prepared by the dip-coating technique. However, the obtained resistivity is one order lower than the recently reported minimum resistivity of  $2 \times 10^{-2} \Omega \text{ cm}$  for 1% Al-doped ZnO films prepared by the sol–gel spin coating technique [22].

Figure 6 shows the  $J$ – $V$ – $L$  and  $J$ – $L$  characteristics of the OLED device measured under forward bias condition.

The inset in figure 6(a) shows the OLED device structure used in this work. The active area of the device was about  $1.4 \times 1.4 \text{ mm}^2$ . Diode-like behaviour is clearly seen from the  $J$ – $V$ – $L$  characteristics in figure 6(a). A luminance of  $1000 \text{ cd m}^{-2}$  was observed at 19 V and at a current density of  $43 \text{ mA cm}^{-2}$ . The lower value of the current density of the OLED in this work may be due to the higher contact resistance resulting from the large difference between the work function of the GZO (4.1 eV [29]) and the HOMO level of m-MTDATA (5.1 eV). The large barrier height reduces the hole injection and hence the performance of the device. It may be mentioned here that after patterning the GZO films, the sheet resistance of the GZO films was found to be increased by up to one order of magnitude. The increase in sheet resistance could be due to our preliminary Kapton tape based patterning method that can damage the surface quality of the GZO film during a removal process. Hence, the performance of the device can be improved by appropriate patterning of the GZO thin films and the surface modification technique by improving the carrier injection properties at the GZO/m-MTDATA interface.

#### 4. Conclusions

In conclusion, Ga-doped ZnO thin films were successfully prepared by a simple sol–gel spin coating technique. XRD results showed preferential  $c$ -axis orientation of the crystallites and the size of the grains was found to decrease with Ga incorporation in the films. A lowest resistivity of  $3.3 \times 10^{-3} \Omega \text{ cm}$  was obtained for the ZnO film doped with 2 at% Ga. All the films showed more than 80% transparency in the entire visible region. The band gap of the Ga-doped ZnO films is blue shifted from that of the undoped ZnO film, which can be explained by the Burstein–Moss effect. The lower current density and luminance of the OLED device are attributed to the larger contact resistance resulting from the difference between the work function of GZO and the HOMO level of m-MTDATA. Further investigations concerning appropriate patterning, surface treatment and different device configurations are presently under consideration. However, the results obtained indicate the possibility that low cost spin-coated Ga-doped ZnO films can be used as transparent conductors for optoelectronic devices.

#### Acknowledgments

This work was supported by the Seoul R&BD Program (CRO70048) and by the BK21 project of the Ministry of Education, Korea. The authors also wish to thank Junhee Cho and Minkyu Kwon for technical assistance.

#### References

- [1] Hartnagel H L, Dawar A L, Jain A K and Jagadish C 1995 *Semiconducting Transparent Thin Films* (Bristol: Institute of Physics Publishing)
- [2] Shen Z, Burrows P E, Bulovic V, Forrest S R and Thompson M E 1997 *Science* **276** 2009
- [3] Bhosle V, Tiwari A and Narayan J 2006 *Appl. Phys. Lett.* **88** 032106

- [4] Guillén C and Herrero J 2006 *Thin Solid Films* **515** 640
- [5] Nunes P, Fortunato E, Tonello P, Fernandes F B, Vilarinho P and Martins R 2002 *Vacuum* **64** 281
- [6] Majumder S B, Jain M, Dobal P S and Katiyar R S 2003 *Mater. Sci. Eng. B* **103** 16
- [7] Kim H, Gilmore C M, Horwitz J S, Piqué A, Murata H, Kushto G P, Schlaf R, Kafafi Z H and Chrisey D B 2000 *Appl. Phys. Lett.* **76** 259
- [8] Yim K, Kim H W and Lee C 2007 *Mater. Sci. Technol.* **23** 108
- [9] Nakagawara O, Kishimoto Y, Seto H, Koshido Y, Yoshino Y and Makino T 2006 *Appl. Phys. Lett.* **89** 091904
- [10] Bolink H J, Coronado E, Repetto D and Sessolo M 2007 *Appl. Phys. Lett.* **91** 223501
- [11] Hu J and Gordon R G 1992 *J. Appl. Phys.* **72** 5381
- [12] Ma Q B, Ye Z Z, He H P, Hu S H, Wang J R, Zhu L P, Zhang Y Z and Zhao B H 2007 *J. Cryst. Growth* **304** 64
- [13] Reddy K T R, Reddy T B S, Forbes I and Miles R W 2002 *Surf. Coat. Technol.* **151** 110
- [14] Kaul A R, Gorbenko OY, Botev A N and Burova L I 2005 *Superlatt. Microstruct.* **38** 272
- [15] Snure M and Tiwari A 2007 *J. Appl. Phys.* **101** 124912
- [16] Ahn B D, Kim J H, Kang H S, Lee C H, Oh S H, Kim K W, Jang G and Lee S Y 2008 *Thin Solid Films* **516** 1382
- [17] Park S M, Ikegami T and Ebihara K 2006 *Thin Solid Films* **513** 90
- [18] Minami T, Ida S, Miyata T and Minamino Y 2003 *Thin Solid Films* **445** 268
- [19] Fathollahi V and Amini M M 2001 *Mater. Lett.* **50** 235
- [20] Iwata K, Sakemi T, Yamada A, Fons P, Awai K, Yamamoto T, Matsubara M, Tampo H and Niki S 2003 *Thin Solid Films* **445** 274
- [21] Nishino J, Ohshio S and Kamata K 1992 *J. Am. Ceram. Soc.* **75** 3469
- [22] Mridha S and Basak D 2007 *J. Phys. D: Appl. Phys.* **40** 6902
- [23] Burstein E 1954 *Phys. Rev.* **93** 632
- [24] Moss T S 1954 *Proc. Phys. Soc. Lond. B* **67** 775
- [25] Liu Y and Lian J 2007 *Appl. Surf. Sci.* **253** 3727
- [26] Hagemark K I and Chacka L C 1975 *J. Solid State Chem.* **15** 261
- [27] Schoenes J, Kanazawa K and Kay E 1977 *J. Appl. Phys.* **48** 2537
- [28] Oba F, Togo A, Tanaka I, Paier J and Kresse G 2008 *Phys. Rev. B* **77** 245202
- [29] Bhosle V, Prater J T, Yang F, Burk D, Forrest S R and Narayan J 2007 *J. Appl. Phys.* **102** 023501